 CMES, vol.99, no.6, pp.473-490, 2014

A Precise Integration Method for Modeling GPR Wave Propagation in Layered Pavement Structure

H. Y. Fang[1,2,3], J. Liu[4] and F. M. Wang[1,2]

Abstract: Construction of electromagnetic wave propagation model in layered pavement structure is a key step in back analysis of ground penetrating radar (GPR) echo signal. The precise integration method (PIM) is a highly accurate, efficient, and unconditionally stable algorithm for solving 1-order ordinary differential equations. It is quite suitable for dealing with problems of wave propagation in layered media. In this paper, forward simulation of GPR electromagnetic wave propagating in homogeneous layered pavement structure is developed by employing PIM. To verify the performance of the proposed algorithm, simulated GPR signal is compared with the measured one. Excellent agreement is achieved.

Keywords: ground penetrating radar, pavement structure, precise integration method, numerical simulation.

1 Introduction

In recent years, ground penetrating radar (GPR) has been widely applied to road quality detection [Hugenschmidt, Partl and de Witte (1998); Grote, Hubbard, Harvey and Rubin (2005); Lahouar and Al-Qadi (2008); Solla, Lorenzo, Rial and Novo(2011)] as is known for speed, high efficiency, and collecting data non-destructively. The layer thickness, water content and other information of the road can be predicted by inverse analysis of GPR echo signal without destroying pavement. However, construction of GPR propagation model for inverse analysis in layered structure pavement is still a challenging task.

Various approaches have been developed to deal with electromagnetic wave propagation in layered media. Yang (1997) developed a spectral recursive transformation

[1] College of Water Conservancy & Environmental Engineering, Zhengzhou University. Zhengzhou 450001, China.

[2] Collaborative Innovation Center of Water Conservancy and Transportation Infrastructure Safety, Henan Province, Zhengzhou 450001, China.

[3] corresponding author. E-mail: fanghongyuan1982@163.com

[4] Faculty of infrastructure engineering, Dalian University of Technology, Dalian 116024, China.

method for plane wave propagation in generalized anisotropic layered media. An inhomogeneous plane wave algorithm in multi-layered media was investigated by Hu and Chew (2000). Zheng and Ge (2000) proposed a transfer matrix method for calculating the reflection and transmission coefficients of anisotropic stratified media. Mosig and Melcon (2003) presented an efficient technique for evaluating Green's functions associated with layered media. A simplified model based on Fast Fourier Transform (FFT) was developed to calculate the reflection coefficients in homogeneous layered media [Zhong, Zhang and Wang (2006)]. Demarest, Plumb and Huang (1995) calculated the reflection and transmission coefficients in a continuous space by finite difference time domain (FDTD) method. Subsequently, the FDTD method was developed to simulate TE and TM plane waves propagating in arbitrary layered media [Winton, Kosmas and Rappaport (2005)]. The GPR propagation model in layered pavement structure was established by Diamanti, Redman and Giannopoulos (2010) using FDTD.

However, there are still some difficulties when applying these models and methods to simulate the GPR wave propagation in pavement structure. For example, the simplified model proposed by Zhong, Zhang and Wang (2006) neglects multiple reflections of electromagnetic wave in layered media. The transfer matrix method is possible to cause numerical instability if materials of layered media are dissipative. The FDTD method is restricted by CFL stability condition, i.e. the maximum time step available is limited by the minimum element size in space domain. In order to acquire high precision, large memory size and significant calculation time are needed.

The precise integration method (PIM) [Zhong (2001)] is a highly accurate and unconditionally stable numerical method for solving first-order liner ordinary differential equations. It can produce numerical results up to the precision of the computer used. The PIM has been successfully applied to solve problems of elastic wave propagation in stratified materials [Gao, Zhong and Howson (2004); Zhong, Lin and Gao (2004); Gao, Lin, Zhong, Howson and Williams (2006); Gao, Lin, Zhong, Howson and Williams (2006)].

In this paper, the Maxwell equations are formulated in the frequency-wavenumber domain as a set of first-order ordinary differential equations containing variables being only the horizontal components of the electric and magnetic fields. Then these equations are solved by PIM with specified two-point boundary value conditions. The performance of the proposed algorithm is verified by comparing the calculated results and measured signals.

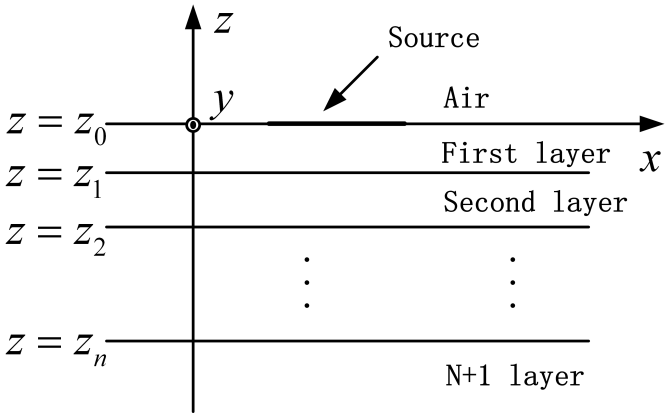

Figure 1: Profile of the layered pavement structure.

2 Formulation of the governing equations

As shown in Fig. 1, the x-axis and y-axis point to the two orthogonal horizontal directions of propagation, and the z-axis points vertically upward. The air layer and the (n+1)th layer are considered as upper and lower infinite space. The incident source is placed at the surface of ground ($z = z_0$).

Without loss of generality, the lossy media are assumed to be anisotropic in this paper. Hence, the Maxwell equations in frequency domain take the following form

$$\nabla \times \mathbf{h} = i\omega \boldsymbol{\varepsilon}' \cdot \mathbf{e} \tag{1}$$

$$\nabla \times \mathbf{e} = -i\omega \boldsymbol{\mu} \cdot \mathbf{h} \tag{2}$$

where $\mathbf{e}$ and $\mathbf{h}$ are the electric and magnetic field vectors; $\varepsilon' = \varepsilon - i\sigma/\omega$ represents the complex permittivity tensor; ε, μ and σ are permittivity, permeability and conductivity tensors, respectively.

In order to facilitate the matching of boundary conditions at the interface between two adjacent layers of a layered system, curl operator and field components are decomposed as follows [Chew (1995)]

$$\nabla = \nabla_s + \widehat{\mathbf{z}}\frac{\partial}{\partial z} \quad , \quad \mathbf{e} = \mathbf{e}_s + \mathbf{e}_z \quad , \quad \mathbf{h} = \mathbf{h}_s + \mathbf{h}_z \tag{3}$$

Then the tensors $\boldsymbol{\varepsilon}'$ and $\boldsymbol{\mu}$ are partitioned as

$$\boldsymbol{\varepsilon}' = \begin{bmatrix} \boldsymbol{\varepsilon}'_s & \boldsymbol{\varepsilon}'_{sz} \\ \boldsymbol{\varepsilon}'_{zs} & \boldsymbol{\varepsilon}'_{zz} \end{bmatrix} \quad \boldsymbol{\mu} = \begin{bmatrix} \boldsymbol{\mu}_s & \boldsymbol{\mu}_{sz} \\ \boldsymbol{\mu}_{zs} & \boldsymbol{\mu}_{zz} \end{bmatrix} \tag{4}$$

where the subscript s and z denote the horizontal component and vertical component, respectively. Moreover, $\boldsymbol{\varepsilon}_s^{'}$ is a 2×2 matrix, $\boldsymbol{\varepsilon}_{sz}^{'}$ is a 2×1 matrix, $\boldsymbol{\varepsilon}_{zs}^{'}$ is a 1×2 matrix, and $\boldsymbol{\varepsilon}_{zz}^{'}$ is a 1×1 matrix. Similar decomposition holds for $\boldsymbol{\mu}$.

Substituting Eq. (3) and Eq. (4) into Eq. (1) and Eq. (2) and removing $\mathbf{h}_z$ and $\mathbf{e}_z$ by expressing them in terms of $\mathbf{h}_s$ and $\mathbf{e}_s$, we have

$$\begin{aligned}\frac{\partial}{\partial z}\mathbf{e}_s =&[(-\widehat{\mathbf{z}}\times\frac{\boldsymbol{\mu}_{sz}}{\boldsymbol{\mu}_{zz}}\nabla_s\times)-(\widehat{\mathbf{z}}\times\nabla_s\times\frac{\boldsymbol{\varepsilon}_{zs}^{'}}{\boldsymbol{\varepsilon}_{zz}^{'}}\cdot)]\mathbf{e}_s\\&+[(i\omega\widehat{\mathbf{z}}\times\mu_s\cdot)-(i\omega\widehat{\mathbf{z}}\times\frac{\boldsymbol{\mu}_{sz}\cdot\boldsymbol{\mu}_{zs}}{\boldsymbol{\mu}_{zz}}\cdot)+(\widehat{\mathbf{z}}\times\nabla_s\times\frac{1}{i\omega\varepsilon_{zz}^{'}}\nabla_s\times)]\mathbf{h}_s\end{aligned} \tag{5}$$

$$\begin{aligned}\frac{\partial}{\partial z}\mathbf{h}_s =&[(-i\omega\widehat{\mathbf{z}}\times\boldsymbol{\varepsilon}_s^{'}\cdot)+(i\omega\widehat{\mathbf{z}}\times\frac{\boldsymbol{\varepsilon}_{sz}^{'}\cdot\boldsymbol{\varepsilon}_{zs}^{'}}{\boldsymbol{\varepsilon}_{zz}^{'}}\cdot)-(\widehat{\mathbf{z}}\times\nabla_s\times\frac{1}{i\omega\boldsymbol{\mu}_{zz}}\nabla_s\times)]\mathbf{e}_s\\&+[(-\widehat{\mathbf{z}}\times\frac{\boldsymbol{\varepsilon}_{sz}^{'}}{\boldsymbol{\varepsilon}_{zz}^{'}}\nabla_s\times)-(\widehat{\mathbf{z}}\times\nabla_s\times\frac{\boldsymbol{\mu}_{zs}}{\boldsymbol{\mu}_{zz}})]\mathbf{h}_s\end{aligned} \tag{6}$$

Moreover, by assuming that the horizontal components of the electric and magnetic field vectors have $\exp(i\mathbf{k_s}\cdot\mathbf{r})$ dependence in the horizontal direction for all z, $\mathbf{e}_s$ and $\mathbf{h}_s$ can be expressed as

$$\mathbf{e}_s(\mathbf{r},\omega)=\mathbf{e}_s(z,\omega)\cdot\exp(i\mathbf{k_s}\cdot\mathbf{r_s})=\mathbf{e}_s(z,\omega)\cdot\exp[i(k_x\cdot x+k_y\cdot y)] \tag{7}$$

$$\mathbf{h}_s(\mathbf{r},\omega)=\mathbf{h}_s(z,\omega)\cdot\exp(i\mathbf{k_s}\cdot\mathbf{r_s})=\mathbf{h}_s(z,\omega)\cdot\exp[i(k_x\cdot x+k_y\cdot y)] \tag{8}$$

Substituting Eq. (7) and Eq. (8) into Eq. (5) and Eq. (6), the governing equations can be written in a matrix form as a state equation in frequency-wavenumber domain.

$$\begin{bmatrix}\mathbf{e}_s^{'}\\ \mathbf{h}_s^{'}\end{bmatrix}=\begin{bmatrix}\mathbf{H}_{11} & \mathbf{H}_{12}\\ \mathbf{H}_{21} & \mathbf{H}_{22}\end{bmatrix}\cdot\begin{bmatrix}\mathbf{e}_s\\ \mathbf{h}_s\end{bmatrix} \tag{9}$$

where $\mathbf{e}_s^{'}=d\mathbf{e}_s\big/dz$; $\mathbf{h}_s^{'}=d\mathbf{h}_s\big/dz$; $\mathbf{e}_s$=$(\mathbf{e}_x,\mathbf{e}_y)$; $\mathbf{h}_s$=$(\mathbf{h}_x,\mathbf{h}_y)$. $\mathbf{H}_{11}$,$\mathbf{H}_{12}$,$\mathbf{H}_{21}$ and $\mathbf{H}_{22}$ are all 2×2 matrices derivable from Eq. (5) and Eq. (6), and the matrices elements are shown in Appendix. To simplify the nomenclature, the subscript s is omitted hereafter.

Equation (9) can be rewritten as

$$\mathbf{v}'=\mathbf{H}\cdot\mathbf{v} \tag{10}$$

where $\mathbf{v}=(\mathbf{e}_x,\mathbf{e}_y,\mathbf{h}_x,\mathbf{h}_y)^T$ is a four-component column vector, and $\mathbf{H}$ is a 4×4 matrix.

The sources are taken as input of electric and magnetic field components at the surface of the layered system (see Fig. 1), and then the following boundary conditions are applied.

$$\begin{aligned}\mathbf{e}(k_x,k_y,\omega,z_0^+)+\mathbf{e}_m(k_x,k_y,\omega)&=\mathbf{e}(k_x,k_y,\omega,z_0^-)\\ \mathbf{h}(k_x,k_y,\omega,z_0^+)+\mathbf{h}_m(k_x,k_y,\omega)&=\mathbf{h}(k_x,k_y,\omega,z_0^-)\end{aligned} \tag{11}$$

where $\mathbf{e}_m$ and $\mathbf{h}_m$ are the input of electric and magnetic field components, i.e. the incident source in frequency-wavenumber domain. z_0^+ and z_0^- represent the upper and lower faces of the interface z_0, respectively.

The governing equations should also satisfy the radiation condition in the semi-infinite space.

The state equation in air layer is expressed as

$$\dot{\mathbf{v}}_0=\mathbf{H}\cdot\mathbf{v}_0 \tag{12}$$

Hence if $\mathbf{T}_0$ and $\mathbf{\Lambda}_0$ are the eigenvector and eigenvalue matrices of matrix $\mathbf{H}$, then

$$\dot{\mathbf{v}}_0=\mathbf{T}_0\mathbf{\Lambda}_0\mathbf{T}_0^{-1}\mathbf{v}_0 \tag{13}$$

where $\mathbf{T}_0$ and $\mathbf{\Lambda}_0$ are all 4×4 matrices, i.e.

$$\mathbf{\Lambda}_0=diag(\lambda_1,\lambda_2,\lambda_3,\lambda_4) \tag{14}$$

$$\mathbf{T}_0=(\alpha_1,\alpha_2,\alpha_3,\alpha_4) \tag{15}$$

in which $\lambda_i(i=1,2,3,4)$is the i-th eigenvalue and α_i is the eigenvector corresponding to λ_i. These eigenvalues and eigenvectors are arranged such that the first two elements of (14) correspond to the upward waves while the last two elements correspond to downward waves.

By letting $\mathbf{b}_0(z)=\mathbf{T}_0^{-1}\mathbf{v}_0(z)$, Eq. (13) can be rewritten as follow

$$\dot{\mathbf{b}}_0=\mathbf{\Lambda}_0\mathbf{b}_0 \tag{16}$$

The solution of Eq. (16) is

$$\mathbf{b}_0(z)=\exp\left[\mathbf{\Lambda}_0(z-z_0)\right]\cdot\mathbf{b}_0(z_0)\qquad z>z_0 \tag{17}$$

where $\mathbf{b}_0(z_0)$ is a 4×1 vector, the first two components of which represent upwards traveling waves and the other two elements represent waves going downward in the semi-infinite space. The radiation condition requires that no downward traveling

waves exist in the upper semi-infinite space, i.e. the last two elements of $\mathbf{b}_0(z_0)$ must be zero. Therefore,

$$\mathbf{v}_0^+ = \left[\begin{array}{cc} \mathbf{T}_{uu} & \mathbf{T}_{ud} \\ \mathbf{T}_{du} & \mathbf{T}_{dd} \end{array} \right] \left\{ \begin{array}{c} \mathbf{b}_u \\ \hline 0 \end{array} \right\} \tag{18}$$

$$\mathbf{e}_0^+ = \mathbf{T}_{uu} \cdot \mathbf{b}_u \quad , \quad \mathbf{h}_0^+ = \mathbf{T}_{du} \cdot \mathbf{b}_u$$

$$\mathbf{h}_0^+ = \mathbf{T}_{du} \cdot \mathbf{T}_{uu}^{-1} \cdot \mathbf{e}_0^+ = \mathbf{R}_u \mathbf{e}_0^+ \quad , \quad \mathbf{R}_u = \mathbf{T}_{du} \cdot \mathbf{T}_{uu}^{-1} \tag{19}$$

where the subscript 0 represents the field value at z_0, $\mathbf{T}_{uu}$, $\mathbf{T}_{ud}$, $\mathbf{T}_{du}$ and $\mathbf{T}_{dd}$ are all 2×2 matrices and can be obtained by partitioning matrix $\mathbf{T}$. Therefore, Eq. (19) is the radiation condition for the upper semi-infinite space.

Analogously, the solution of the state equation in the lower semi-infinite space, i.e. the (n+1)th layer, may also be expressed as

$$\mathbf{b}_{n+1}(z) = \exp\left[\mathbf{\Lambda}_n(z_n - z)\right] \cdot \mathbf{b}_n(z_n) \qquad z < z_n \tag{20}$$

The radiation condition requires that no upper traveling waves exist in the lower semi-infinite space, i.e. the first two elements of $\mathbf{b}_n(z_n)$ must be zero. Therefore,

$$\mathbf{v}_n^- = \left[\begin{array}{cc} \mathbf{T}_{uu} & \mathbf{T}_{ud} \\ \mathbf{T}_{du} & \mathbf{T}_{dd} \end{array} \right] \left\{ \begin{array}{c} 0 \\ \hline \mathbf{b}_d \end{array} \right\} \tag{21}$$

$$\mathbf{e}_n^- = \mathbf{T}_{ud} \cdot \mathbf{b}_d, \quad \mathbf{h}_n^- = \mathbf{T}_{dd} \cdot \mathbf{b}_d$$

$$\mathbf{h}_n^- = \mathbf{T}_{dd} \cdot \mathbf{T}_{ud}^{-1} \cdot \mathbf{e}_n^- = \mathbf{R}_d \mathbf{e}_n^-, \quad \mathbf{R}_d = \mathbf{T}_{dd} \cdot \mathbf{T}_{ud}^{-1} \tag{22}$$

Thus, Eq. (22) is the radiation condition for the lower semi-infinite space.

The continuous conditions at the interfaces between two adjacent layers are

$$\mathbf{e}(z = z_i^+) = \mathbf{e}(z = z_i^-), \mathbf{h}(z = z_i^+) = \mathbf{h}(z = z_i^-) \qquad (i = 1, 2, \cdots, n) \tag{23}$$

3 The precise integration method for solving two-point boundary value problem

The transfer matrix method is usually employed in solving the Eq. (10) for layered case. Select an interval $[Z_a, Z_b]$ within an arbitrary layer. The relationship of the field values at two ends of the interval can be expressed as

$$\mathbf{v}_b = \exp(\mathbf{H}_{ba} \cdot (z_b - z_a)) \cdot \mathbf{v}_a = \mathbf{P}_b(z_b, z_a) \cdot \mathbf{v}_a \tag{24}$$

where $\mathbf{v}_a$ and $\mathbf{v}_b$ represent the field values at z_a and z_b, respectively. The matrix $\mathbf{P}$ is also known as the transfer matrix, relating the state vectors that describe the fields at two different locations z_a and z_b.

Then the transfer matrix of the global interval $[z_0, z_n]$ can be obtained by

$$\begin{aligned}\mathbf{v}_n &= \mathbf{P}_n(z_n, z_{n-1}) \cdot \mathbf{v}_{n-1} \\ &= \mathbf{P}_n(z_n, z_{n-1}) \cdot \mathbf{P}_{\mathbf{n-1}}(z_{n-1}, z_{n-2}) \cdot \mathbf{v}_{n-2} = \cdots = \prod_{i=1}^{n} \mathbf{P}_i(z_i, z_{i-1}) \cdot \mathbf{v}_0\end{aligned} \tag{25}$$

However if media are lossy, Eq. (25) implies that the matrix **P** may have exponentially large terms as well as exponentially small terms. The existence of these exponentially large terms could make the method unstable. Alternatively, the precise integration approach is proposed.

In fact, for linear systems, the following relations of the field values at the two ends of arbitrary interval $[z_a, z_b]$ stand

$$\mathbf{e}_b = \mathbf{F}\mathbf{e}_a - \mathbf{G}\mathbf{h}_b \tag{26}$$

$$\mathbf{h}_a = \mathbf{Q}e_a + \mathbf{E}\mathbf{h}_b \tag{27}$$

where **E**, **F**, **G** and **Q** are all 2×2 complex matrices to be determined, which are only depending on z_a and z_b.

In order to obtain exact expressions of matrices **E**, **F**, **G** and **Q**, in the PIM, the thickness of a typical layer $h_r = z_r - z_{r-1}\,(r = 1, 2, \cdots n+1)$ is firstly divided into $2^{N_1}(N_1 = 6$in this paper) sub-layers of equal thickness; then, each sub-layer is further divided into $2^{N_2}(N_2 = 20$ in this paper) mini-layers with equal thickness τ. Since τ of the such interval (mini-layer) is extremely small, the associated matrices **E**, **F**, **G** and **Q** can be found in terms of Taylor's series expansion. With increasing terms of Taylor's expansion or powers of τ, any desired accuracy of the results can be reached. In this paper, four terms expansion of Taylor's series is considered sufficiently. As all intervals have equal thickness and identical material constants, combination of intervals can be performed easily. For each round, two adjacent intervals are combined together, and each pass of combinations can reduce the number of total intervals by a half. In the following paragraphs, formula for combination of the adjacent intervals and calculation of matrices **E**, **F**, **G** and **Q** for initial interval are derived.

3.1 The differential equations of matrices **E, F, G** *and* **Q**

Differentiating Eq. (26) and Eq. (27) with respect to Z_b yields

$$\mathbf{e}_b^{'} = \mathbf{F}^{'}\mathbf{e}_a - \mathbf{G}^{'}\mathbf{h}_b - \mathbf{G}\mathbf{h}_b^{'} \tag{28}$$

$$0 = \mathbf{Q}^{'}\mathbf{e}_a + \mathbf{E}^{'}\mathbf{h}_b + \mathbf{E}\mathbf{h}_b^{'} \tag{29}$$

At z_b, Eq. (9) can be written as

$$\mathbf{e}_b^{'} = \mathbf{H}_{11}\mathbf{e}_b + \mathbf{H}_{12}\mathbf{h}_b \tag{30}$$

$$\mathbf{h}_b^{'} = \mathbf{H}_{21}\mathbf{e}_b + \mathbf{H}_{22}\mathbf{h}_b \tag{31}$$

Combining Eq. (26)-Eq. (31), one obtains

$$(\mathbf{F}^{'} - \mathbf{H}_{11}\mathbf{F} - \mathbf{G}\mathbf{H}_{21}\mathbf{F})e_a + (-\mathbf{G}^{'} - \mathbf{H}_{12} - \mathbf{G}\mathbf{H}_{22} + \mathbf{H}_{11}\mathbf{G} + \mathbf{G}\mathbf{H}_{21}\mathbf{G})\mathbf{h}_b = 0 \tag{32}$$

$$(\mathbf{Q}^{'} + \mathbf{E}\mathbf{H}_{21}\mathbf{F})e_a + (-\mathbf{E}\mathbf{H}_{21}\mathbf{G} + \mathbf{E}^{'} + \mathbf{E}\mathbf{H}_{22})\mathbf{h}_b = 0 \tag{33}$$

Note that the vectors $\mathbf{e}_a$ and $\mathbf{h}_b$ are mutually independent, which leads to

$$\begin{aligned} \mathbf{F}^{'} &= \mathbf{H}_{11}\mathbf{F} + \mathbf{G}\mathbf{H}_{21}\mathbf{F} \\ \mathbf{E}^{'} &= \mathbf{E}\mathbf{H}_{21}\mathbf{G} - \mathbf{E}\mathbf{H}_{22} \\ \mathbf{G}^{'} &= -\mathbf{H}_{12} - \mathbf{G}\mathbf{H}_{22} + \mathbf{H}_{11}\mathbf{G} + \mathbf{G}\mathbf{H}_{21}\mathbf{G} \\ \mathbf{Q}^{'} &= -\mathbf{E}\mathbf{H}_{21}\mathbf{F} \end{aligned} \tag{34}$$

The boundary conditions for these equations are derived by letting z_a approach z_b.

$$\begin{aligned} &\mathbf{G}(z_a, z_b) = \mathbf{Q}(z_a, z_b) = 0 \\ &\mathbf{F}(z_a, z_b) = \mathbf{E}(z_a, z_b) = \mathbf{I} \end{aligned} \tag{35}$$

Equation (34) defines the differential equations for matrices **E**, **F**, **G** and **Q** of the interval $[z_a, z_b]$.

3.2 The combination of adjacent intervals

Applying Eq. (26) and Eq. (27) to two adjacent intervals$[z_a, z_b]$and$[z_b, z_c]$gives

$$\mathbf{e}_b = \mathbf{F}_1\mathbf{e}_a - \mathbf{G}_1\mathbf{h}_b \tag{36}$$

$$\mathbf{h}_a = \mathbf{Q}_1\mathbf{e}_a + \mathbf{E}_1\mathbf{h}_b \tag{37}$$

$$\mathbf{e}_c = \mathbf{F}_2\mathbf{e}_b - \mathbf{G}_2\mathbf{h}_c \tag{38}$$

$$\mathbf{h}_b = \mathbf{Q}_2\mathbf{e}_b + \mathbf{E}_2\mathbf{h}_c \tag{39}$$

Using Eq. (26) and Eq. (27) to the combined interval $[z_a, z_c]$ yields

$$\mathbf{e}_c = \mathbf{F}_c\mathbf{e}_a - \mathbf{G}_c\mathbf{h}_c \tag{40}$$

$$\mathbf{h}_a = \mathbf{Q}_c\mathbf{e}_a + \mathbf{E}_c\mathbf{h}_c \tag{41}$$

Substituting Eq. (39) into Eq. (36) leads to

$$\mathbf{e}_b = (\mathbf{I} + \mathbf{G}_1\mathbf{Q}_2)^{-1}\mathbf{F}_1\mathbf{e}_a - (\mathbf{G}_1^{-1} + \mathbf{Q}_2)^{-1}\mathbf{E}_2\mathbf{h}_c \tag{42}$$

Using Eq. (36) and Eq. (39), $\mathbf{h}_b$ is solved as

$$\mathbf{h}_b = (\mathbf{Q}_2^{-1} + \mathbf{G}_1)^{-1}\mathbf{F}_1\mathbf{e}_a - (\mathbf{I} + \mathbf{Q}_2\mathbf{G}_1)^{-1}\mathbf{E}_2\mathbf{h}_c \tag{43}$$

Substituting Eq. (39) and Eq. (42) into Eq. (37) and Eq. (40) leads to

$$\begin{aligned} \mathbf{e}_c &= \mathbf{F}_2(\mathbf{I} + \mathbf{G}_1\mathbf{Q}_2)^{-1}\mathbf{F}_1\mathbf{e}_a - [\mathbf{G}_2 + \mathbf{F}_2(\mathbf{G}_1^{-1} + \mathbf{Q}_2)^{-1}\mathbf{E}_2]\mathbf{h}_c \\ \mathbf{h}_a &= [\mathbf{Q}_1 + \mathbf{E}_1(\mathbf{Q}_2^{-1} + \mathbf{G}_1)^{-1}\mathbf{F}]\mathbf{e}_a + \mathbf{E}_1(\mathbf{I} + \mathbf{Q}_2\mathbf{G}_1)^{-1}\mathbf{E}_2\mathbf{h}_c \end{aligned} \tag{44}$$

Comparing Eq. (40) and Eq. (41) with Eq. (44) gives the combined matrices with subscript$c$.

$$\begin{aligned} \mathbf{F}_c &= \mathbf{F}_2(\mathbf{I} + \mathbf{G}_1\mathbf{Q}_2)^{-1}\mathbf{F}_1 \\ \mathbf{G}_c &= \mathbf{G}_2 + \mathbf{F}_2(\mathbf{G}_1^{-1} + \mathbf{Q}_2)^{-1}\mathbf{E}_2 \\ \mathbf{Q}_c &= \mathbf{Q}_1 + \mathbf{E}_1(\mathbf{Q}_2^{-1} + \mathbf{G}_1)^{-1}\mathbf{F} \\ \mathbf{E}_c &= \mathbf{E}_1(\mathbf{I} + \mathbf{Q}_2\mathbf{G}_1)^{-1}\mathbf{E}_2 \end{aligned} \tag{45}$$

3.3 Calculation of initial interval matrices

Four terms expansion of Taylor's series is assumed for the matrices of initial mini-layer.

$$\begin{aligned} \mathbf{Q}(\tau) &= \theta_1\tau + \theta_2\tau^2 + \theta_3\tau^3 + \theta_4\tau^4 \\ \mathbf{G}(\tau) &= \gamma_1\tau + \gamma_2\tau^2 + \gamma_3\tau^3 + \gamma_4\tau^4 \\ \mathbf{F}'(\tau) &= \phi_1\tau + \phi_2\tau^2 + \phi_3\tau^3 + \phi_4\tau^4 \quad , \quad \mathbf{F}(\tau) = \mathbf{I} + \mathbf{F}'(\tau) \\ \mathbf{E}'(\tau) &= \psi_1\tau + \psi_2\tau^2 + \psi_3\tau^3 + \psi_4\tau^4 \quad , \quad \mathbf{E}(\tau) = \mathbf{I} + \mathbf{E}'(\tau) \end{aligned} \tag{46}$$

where $\boldsymbol{\theta}_i$, $\boldsymbol{\gamma}_i$, $\boldsymbol{\phi}_i$, $\boldsymbol{\psi}_i (i = 1,2,3,4)$ are all 2×2 complex matrices, and $\mathbf{I}$ is a 2×2 unit matrix.

Substituting Eq. (46) into Eq. (34) and comparing coefficients of each power term of τ, we have

$$\begin{aligned} &\theta_1 = -\mathbf{H}_{21}, \gamma_1 = -\mathbf{H}_{12}, \phi_1 = \mathbf{H}_{11}, \psi_1 = -\mathbf{H}_{22} \\ &\theta_2 = -(\psi_1\mathbf{H}_{21} + \mathbf{H}_{21}\phi_1)/2, \qquad \gamma_2 = (\mathbf{H}_{11}\gamma_1 - \gamma_1\mathbf{H}_{22})/2 \\ &\phi_2 = (\mathbf{H}_{11}\phi_1 + \gamma_1\mathbf{H}_{21})/2, \qquad \psi_2 = (\mathbf{H}_{21}\gamma_1 - \psi_1\mathbf{H}_{22})/2 \\ &\theta_3 = -(\psi_2\mathbf{H}_{21} + \mathbf{H}_{21}\phi_2 + \psi_1\mathbf{H}_{21}\phi_1)/3, \qquad \gamma_3 = (\mathbf{H}_{11}\gamma_2 - \gamma_2\mathbf{H}_{22} + \gamma_1\mathbf{H}_{21}\gamma_1)/3 \\ &\phi_3 = (\mathbf{H}_{11}\phi_2 + \gamma_2\mathbf{H}_{21} + \gamma_1\mathbf{H}_{21}\phi_1)/3, \qquad \psi_3 = (\mathbf{H}_{21}\gamma_2 + \psi_1\mathbf{H}_{21}\gamma_1 - \psi_2\mathbf{H}_{22})/3 \end{aligned} \tag{47}$$

$$\theta_4 = -(\psi_3\mathbf{H}_{21} + \mathbf{H}_{21}\phi_3 + \psi_2\mathbf{H}_{21}\phi_1 + \psi_1\mathbf{H}_{21}\phi_2)/4$$

$$\gamma_4 = (\mathbf{H}_{11}\gamma_3 - \gamma_3\mathbf{H}_{22} + \gamma_2\mathbf{H}_{21}\gamma_1 + \gamma_1\mathbf{H}_{21}\gamma_2)/4$$

$$\phi_4 = (\mathbf{H}_{11}\phi_3 + \gamma_3\mathbf{H}_{21} + \gamma_2\mathbf{H}_{21}\phi_1 + \gamma_1\mathbf{H}_{21}\phi_2)/4$$

$$\psi_4 = (\mathbf{H}_{21}\gamma_3 + \psi_1\mathbf{H}_{21}\gamma_2 + \psi_2\mathbf{H}_{21}\gamma_1 - \psi_3\mathbf{H}_{22})/4$$

Note that $\mathbf{E}(\tau) = \mathbf{I} + \mathbf{E}'(\tau)$ and $\mathbf{F}(\tau) = \mathbf{I} + \mathbf{F}'(\tau)$, in which $\mathbf{E}'(\tau)$ and $\mathbf{F}'(\tau)$ are very small in the mini-layer because τ is extremely small. $\mathbf{E}'(\tau)$ and $\mathbf{F}'(\tau)$ must be computed and stored independently to avoid loss of the effective digits. Therefore, Eq. (45) is necessary to be replaced by

$$\mathbf{F}_c^{'} = (\mathbf{F}^{'} - \mathbf{GQ}/2)(\mathbf{I}+\mathbf{GQ})^{-1} + (\mathbf{I}+\mathbf{GQ})^{-1}(\mathbf{F}^{'} - \mathbf{GQ}/2) + \mathbf{F}^{'}(\mathbf{I}+\mathbf{GQ})^{-1}\mathbf{F}^{'}$$

$$\mathbf{E}_c^{'} = (\mathbf{E}^{'} - \mathbf{GQ}/2)(\mathbf{I}+\mathbf{GQ})^{-1} + (\mathbf{I}+\mathbf{GQ})^{-1}(\mathbf{F}^{'} - \mathbf{GQ}/2) + \mathbf{E}^{'}(\mathbf{I}+\mathbf{GQ})^{-1}\mathbf{E}^{'} \quad (48)$$

$$\mathbf{G}_c = \mathbf{G} + (\mathbf{I}+\mathbf{F}^{'})(\mathbf{G}^{-1} + \mathbf{Q})^{-1}(\mathbf{I}+\mathbf{E}^{'})$$

$$\mathbf{Q}_c = \mathbf{Q} + (\mathbf{I}+\mathbf{E}^{'})(\mathbf{Q}^{-1} + \mathbf{G}_1)^{-1}(\mathbf{I}+\mathbf{F}^{'})$$

So far, matrices $\mathbf{E}_i$, $\mathbf{F}_i$, $\mathbf{G}_i$ and $\mathbf{Q}_i (i = 1, 2, \cdots, n+1)$ have been obtained for all layers. **Ec**, **Fc**, **Gc** and **Qc** of the whole domain $\left[z_0^-, z_n^+\right]$ are combined using Eq. (45) analogously.

Substituting the matrices **Ec**, **Fc**, **Gc** and **Qc** into Eq. (26) and Eq. (27), the dual equations of the domain $\left[z_0^-, z_n^+\right]$ are obtained.

$$\mathbf{e}_n^+ = \mathbf{Fc}\cdot\mathbf{e}_0^- - \mathbf{Gc}\cdot\mathbf{h}_n^+ \quad (49)$$

$$\mathbf{h}_0^- = \mathbf{Qc}\cdot e_0^- + \mathbf{Ec}\cdot\mathbf{h}_n^+ \quad (50)$$

Considering the input source (11) and the corresponding boundary conditions (19) and (22), the above equations can be written as

$$\mathbf{e}_n^+ = \mathbf{Fc}\cdot\mathbf{e}_0^+ - \mathbf{Gc}\cdot\mathbf{R}_d\cdot\mathbf{e}_n^+ + \mathbf{Fc}\cdot\mathbf{e}_m \quad (51)$$

$$\mathbf{R}_u\cdot\mathbf{e}_0^+ = \mathbf{Qc}\cdot\mathbf{e}_0^+ + \mathbf{Ec}\cdot\mathbf{R}_d\cdot\mathbf{e}_n^+ + \mathbf{Qc}\cdot\mathbf{e}_m - \mathbf{h}_m \quad (52)$$

Equations (51) and (52) are the algebraic equations for the evaluation of reflected signals $\mathbf{e}_0^+$ and transmission signals $\mathbf{e}_n^+$ subjected to the incident signal $\mathbf{e}_m$ in the frequency domain.

Time domain analysis of $\mathbf{e}_0^+(t)$ and $\mathbf{e}_n^+(t)$ can be carried out with the aid of Fast Fourier Transform and Inverse Fast Fourier Transform.

4 Numerical examples

Performance of the proposed approach is checked by numerical examples. In the first example the analytical solutions are available. Calculated results of the reflection and transmission coefficients are compared with the results obtained by the analytical means. In the second example, a real time history of input and reflected signal collected at the field are used as the reference to asses the suitability of the model to simulate the multi-layered pavement structure.

Example 1. Reflection and transmission coefficients from a two-layer model

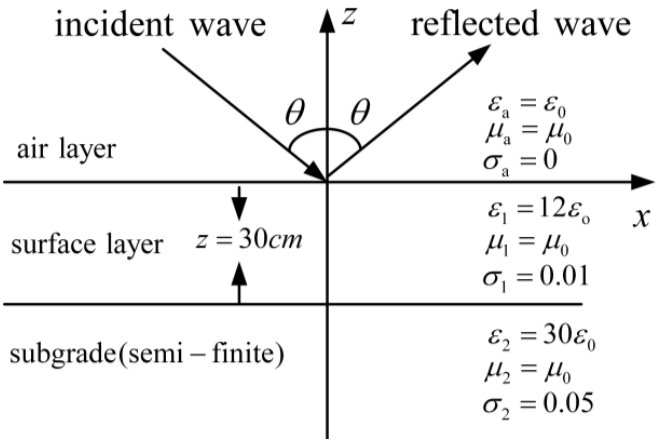

Figure 2: Plane wave reflected and transmitted from a two-layer model.

As shown in Fig. 2, a uniform plane wave is incident upon an isotropic two-layer model in the $x-z$ plane alone. Material electric constants are also specified in the figure, where ε, σ and μ denote permittivity, conductivity and permeability of the media, respectively. It is well known that any plane wave can be decomposed into TE and TM waves in the isotropic media. Therefore, the Eq. (9) can be divided into two groups as shown below:

$$\text{TE waves:} \quad \begin{bmatrix} \mathbf{e}_x' \\ \mathbf{h}_y' \end{bmatrix} = \begin{bmatrix} \mathbf{H}_{11}(1,1) & \mathbf{H}_{12}(1,2) \\ \mathbf{H}_{21}(2,1) & \mathbf{H}_{22}(2,2) \end{bmatrix} \cdot \begin{bmatrix} \mathbf{e}_x \\ \mathbf{h}_y \end{bmatrix} \tag{53}$$

$$\text{TM waves:} \quad \begin{bmatrix} \mathbf{e}_y' \\ \mathbf{h}_x' \end{bmatrix} = \begin{bmatrix} \mathbf{H}_{11}(2,2) & \mathbf{H}_{12}(2,1) \\ \mathbf{H}_{21}(1,2) & \mathbf{H}_{22}(1,1) \end{bmatrix} \cdot \begin{bmatrix} \mathbf{e}_y \\ \mathbf{h}_x \end{bmatrix} \tag{54}$$

For the TM waves, the incident wave can be represented by

$$\begin{aligned} \mathbf{e}_m(x,z) &= \mathbf{e}_{inc}\exp(ik_0 z\cos\theta - ik_0 x\sin\theta) \\ h_m(z) &= h_{inc}\exp(ik_0 z) \end{aligned} \tag{55}$$

where e_{inc} and h_{inc} are amplitudes of the incident waves and θ is the angle of the incidence depicted in Fig. 2. Obviously, to ensure the continuity at the interfaces perpendicular to the z-axis, the total field must have a common factor $\mathbf{e}_{inc}e^{-ik_0 x\sin\theta}$. As a result, the matrix $\mathbf{H}$ of Eq. (54) can be simplified as

$$\mathbf{H}_{12}(2,1) = i\omega\mu, \quad \mathbf{H}_{21}(1,2) = -k_0^2\sin^2\theta/i\omega\mu + i\omega\varepsilon',$$

$$\mathbf{H}_{11}(2,2) = 0, \quad \mathbf{H}_{22}(1,1) = 0$$

Consequently, the reflection and transmission coefficients are defined as

$$R = e_0^+/e_m, \quad T = e_n^+/e_m \tag{56}$$

The calculated reflection and transmission coefficients for incident wave with frequencies $\omega = 0.1,\ 0.5,\ 1.0,\ 1.5,\ 2.0$ and $2.5GHz$ at normal incidence ($\theta = 0^\circ$) are summarized in Table 1 and Table 2, respectively.

Table 1: Reflection coefficients from a two-layer model.

Frequency	Real part		Imaginary part	
(GHz)	Analytical	PIM	Analytical	PIM
0.1	-0.742372	-0.742372	0.206031	0.206031
0.5	-0.441921	-0.441921	-0.032539	-0.032539
1	-0.637720	-0.637720	0.082940	0.082940
1.5	-0.499626	-0.499626	-0.095464	-0.095464
2	-0.586934	-0.586934	0.113660	0.113660
2.5	-0.571497	-0.571497	-0.103555	-0.103555

As shown in Table 1 and Table 2, the numerical results obtained by proposed PIM are identical with those obtained by analytical solutions up to six effective digits.

Example 2. An actual field test

An input signal was collected on a highway site in Henan Province of China generated by an air-coupled surface-radar operated at 1GHz center frequency. The designed geometry of the profile of highway is shown in Table 3. The GPR incident signal was recovered by placing a sufficiently large metal plate under the

Table 2: Transmission coefficients from a two-layer model.

Frequency	Real part		Imaginary part	
(GHz)	Analytical	PIM	Analytical	PIM
0.1	0.213792	0.213792	0.036695	0.036695
0.5	-0.031594	-0.031594	-0.312797	-0.312797
1.0	-0.269328	-0.269328	0.055547	0.055547
1.5	0.154807	0.154807	0.264752	0.264752
2.0	0.248257	0.248257	-0.146309	-0.146310
2.5	-0.223299	-0.223299	-0.186107	-0.186107

antenna. Fig. 3 depicts the GPR incident pulse, which the coupling pulse has been removed and then multiplied by -1 (the reflection coefficient of metal). Subsequently, frequency domain versions of the incident signal$e_m$are obtained via Fast Fourier Transform (FFT).

Table 3: The designed geometry of the profile of a fourlayer pavement structure.

Layer	Material	Thickness(m)
1 Surface	asphalt concrete	0.2
2 Base	cement stabilized macadam	0.2
3 Subbase	lime soil	0.35
4 Subgrade	soil	semi-infinite

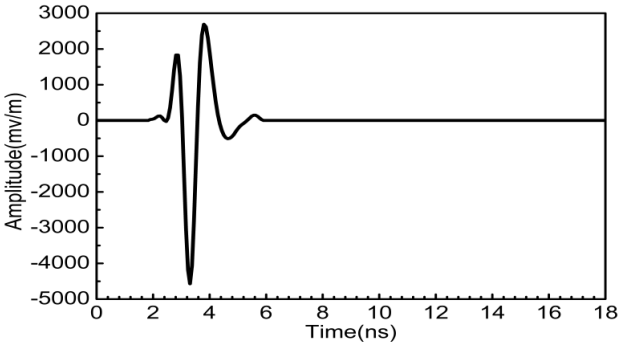

Figure 3: Time history of GPR incident wave.

It is well known that material electric constants of such multi-layered pavement structure can be predicted by inverse analysis based on forward model. For this case, the pavement materials are modeled as homogeneous and nonmagnetic, and system identification back-calculation [Zhong, Wang, Zhang and Cai (2004)] combined with PIM forward simulation scheme is suggested for the evaluation of the electric constants of the pavement materials (shown in Fig. 4).

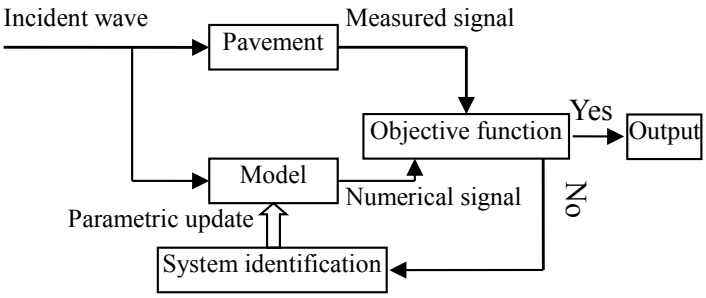

Figure 4: The basic principle of system identification inverse analysis.

Predicted results of electric constants of the pavement materials are collected in Table 4. Fig. 5 shows comparison between the simulated waveform by PIM and signal measured by GPR in the field.

Table 4: Predicted electric constants of fourlayer pavement structure.

Layer	Permittivity(F/m)	Conductivity(S/m)
1	6.5 ε_0	0.01
2	10.5 ε_0	0.02
3	13.0 ε_0	0.05
4	30.0 ε_0	0.05

As can be observed in Fig. 5, simulated waveform fits well with the measured signal in many aspects, such as the peak amplitude and time delay, etc.

In order to verify the efficiency of the PIM, the computer time consumed by PIM and that by one-dimensional FDTD scheme with the 1-order Mur absorbing boundary condition are compared [Sullivan (2000)]. In FDTD scheme, the time step and spatial cell size are chosen as 5×10^{-12}s and 5×10^{-3}m. For one round computation of wave propagation from the instant of input to that of reflection at the surface of the pavement, the computer time needed for PIM herein and that consumed by

FDTD method are 0.09375s and 0.14063s to reach the same level of accuracy, respectively. The PIM approach can save computer time considerably.

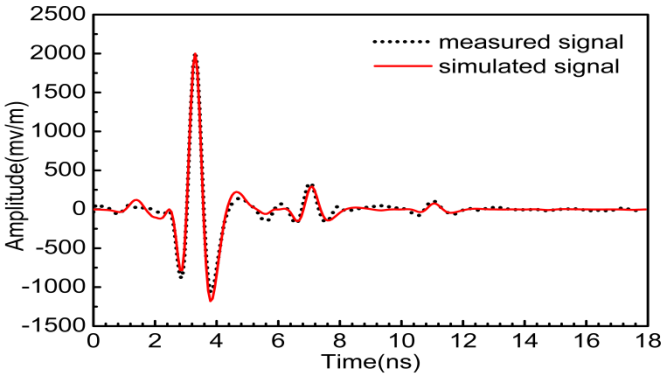

Figure 5: Comparison between the reflected waveform simulated by PIM and that measured by GPR in the field.

5 Conclusion

This paper presents theory and numerical solution procedure for modeling GPR wave propagation in layered pavement structure. The precise integration scheme with two-point boundary value conditions is proposed to solve the governing equations formulated as the 1-order ordinary differential equations. The PIM has the advantage that any desired accuracy can be achieved, because its precision is only limited by the precision of the computer used. Numerical examples are provided to verify the efficiency and accuracy of the proposed approach. If the input and reflected radar wave signals are collected in the field, the material electric constants of the multi-layered pavement structure can be predicted by inverse analysis.

Acknowledgement: This research was supported by China Postdoctoral Science Foundation (Grant No.: 2013M541996) and the Plan for Scientific Innovation Talent of Henan Province (Grant No.: 124200510020), for which the authors are grateful.

Reference

Chew, W. C. (1995): *Waves and fields in inhomogeneous media*. IEEE Press.

Demarest, K.; Plumb, R.; Huang, Z. B. (1995): FDTD modeling of scatters in stratified media. *IEEE Transactions on Antennas and Propagation*, vol. 43, no. 10,

pp. 1164–1168.

Diamanti, N.; Redman, D.; Giannopoulos, A. (2010): A study of GPR vertical crack responses in pavement using field data and numerical modeling. *In: Proceedings of the 13th International Conference on Ground Penetrating Radar, GPR 2010*, Piscataway, NJ, , pp. 1–6.

Hu, B.; Chew, W. C. (2000): Fast inhomogeneous plane wave algorithm for multilayered medium problems. *In: IEEE Antennas and Propagation Society International Symposium: Transmitting Waves of Progress to the Next Millennium*, Piscataway, NJ, pp. 606–609.

Hugenschmidt, J.; Partl, M. N.; de Witte, H. (1998): GPR inspection of a mountain motorway in Switzerland. *Journal of Applied Geophysics*, vol. 40, no. 1-3, pp. 95–104.

Gao, Q.; Zhong, W. X.; Howson, W. P. (2004): A precise method for solving wave propagation problems in layered anisotropic media. *Wave Motion*, vol. 40, no. 3, pp. 191–207.

Gao, Q.; Lin, J. H.; Zhong, W. X.; Howson, W. P.; Williams, F. W. (2006): Random wave propagation in a viscoelastic layered half space. *International Journal of Solids and Structures*, vol. 43, no. 21, pp. 6453–6471.

Gao, Q.; Lin, J. H.; Zhong, W. X.; Howson, W. P.; Williams, F. W. (2006): The precise method for Rayleigh waves in stratified solids. *International Journal for Numerical Methods in Engineering*, vol. 67, no. 6, pp. 771–786.

Grote, K.; Hubbard, S.; Harvey, J.; Rubin, Y. (2005): Evaluation of infiltration in layered pavements using surface GPR reflection techniques. *Journal of Applied Geophysics*, vol. 57, no. 2, pp. 129–153.

Lahouar, S.; Al-Qadi, I. L. (2008): Automatic detection of multiple pavement layers from GPR data. *NDT & E International*, vol. 41, no. 2, pp. 69–81.

Mosig, J. R.; Melcon, A. A. (2003): Green's Functions in lossy layered media: integration along the imaginary axis and asymptotic behavior. *IEEE Transactions on Antennas and Propagation*, vol. 51, no. 12, pp. 3200–3208.

Sullivan, D. M. (2000): *Electromagnetic simulation using the FDTD method*. IEEE Press.

Solla, M.; Lorenzo, H.; Rial, F. I.; Novo, A. (2011): GPR evaluation of the Roman masonry arch bridge of Lugo (Spain). *NDT and E International*, vol. 44, no. 1, pp. 8–12.

Winton, S. C.; Kosmas, P.; Rappaport, C. M. (2005): FDTD Simulation of TE and TM Plane Waves at Nonzero Incidence in Arbitrary Layered Media. *IEEE Transactions on Antennas and Propagation*, vol. 53, no. 5, pp. 1721–1728.

Yang, H. Y. (1997): A spectral recursive transformation method for electromagnetic waves in generalized anisotropic layered media. *IEEE Transactions on Antennas and Propagation*, vol. 45, no. 3, pp. 520–526.

Zheng, H. X.; Ge, D. B. (2000): Electromagnetic wave reflection and transmission of anisotropic layered media by generalized propagation matrix method. *Acta Physica Sinica*, vol. 49, no. 9, pp. 1702–1706.

Zhong, W. X. (2001): Combined method for the solution of asymmetric Riccati differential equations. *Computer Methods in Applied Mechanics and Engineering*, vol. 191, no. 1–2, pp. 93–102.

Zhong, Y. H.; Wang, F. M.; Zhang, B.; Cai, Y. C. (2004): System identification method for evaluating the effect of thickness error on backcalculated pavement layer moduli. *Shanghai Jiaotong Daxue Xuebao*, vol. 38, no. suppl, pp. 182–187.

Zhong, W. X.; Lin, J. H.; Gao, Q. (2004): The precise computation for wave propagation in a stratified materials. *Journal for Numerical Methods in Engineering*, vol. 60, no. 1, pp. 11–25.

Zhong, Y. H.; Zhang, B.; Wang, F. M. (2006): Numerical simulation of ground penetrating radar wave propagation in multi-layered medium. *Journal of Dalian University of Technology*, vol. 46, no. 5, pp. 726–729.

Appendix

Matrices elements of $\mathbf{H}_{11}$, $\mathbf{H}_{12}$, $\mathbf{H}_{21}$ and $\mathbf{H}_{22}$

$$\mathbf{H}_{11}(1,1) = -ik_x\varepsilon'_{zx}\Big/\varepsilon'_{zz} - ik_y\mu_{yz}/\mu_{zz}$$

$$\mathbf{H}_{11}(1,2) = -ik_x\varepsilon'_{zy}\Big/\varepsilon'_{zz} + ik_x\mu_{yz}/\mu_{zz}$$

$$\mathbf{H}_{11}(2,1) = -ik_y\varepsilon'_{zx}\Big/\varepsilon'_{zz} + ik_y\mu_{xz}/\mu_{zz}$$

$$\mathbf{H}_{11}(2,2) = -ik_y\varepsilon'_{zy}\Big/\varepsilon'_{zz} - ik_x\mu_{xz}/\mu_{zz}$$

$$\mathbf{H}_{12}(1,1) = k_xk_y\Big/i\omega\varepsilon'_{zz} - i\omega\mu_{yx} + i\omega\mu_{yz}\mu_{zx}/\mu_{zz}$$

$$\mathbf{H}_{12}(1,2) = -k_xk_x\Big/i\omega\varepsilon'_{zz} - i\omega\mu_{yy} + i\omega\mu_{yz}\mu_{zy}/\mu_{zz}$$

$$\mathbf{H}_{12}(2,1) = k_yk_y\Big/i\omega\varepsilon'_{zz} + i\omega\mu_{xx} - i\omega\mu_{xz}\mu_{zx}/\mu_{zz}$$

$$\mathbf{H}_{12}(2,2) = -k_yk_x\Big/i\omega\varepsilon'_{zz} + i\omega\mu_{xy} - i\omega\mu_{xz}\mu_{zy}/\mu_{zz}$$

$$\mathbf{H}_{21}(1,1) = -k_x k_y / i\omega\mu_{zz} + i\omega\varepsilon'_{yx} - i\omega\varepsilon'_{yz}\varepsilon'_{zx} \Big/ \varepsilon'_{zz}$$

$$\mathbf{H}_{21}(1,2) = k_x k_x / i\omega\mu_{zz} + i\omega\varepsilon'_{yy} - i\omega\varepsilon'_{yz}\varepsilon'_{zy} \Big/ \varepsilon'_{zz}$$

$$\mathbf{H}_{21}(2,1) = -k_y k_y / i\omega\mu_{zz} - i\omega\varepsilon'_{xx} + i\omega\varepsilon'_{xz}\varepsilon'_{zx} \Big/ \varepsilon'_{zz}$$

$$\mathbf{H}_{21}(2,2) = k_y k_x / i\omega\mu_{zz} - i\omega\varepsilon'_{xy} + i\omega\varepsilon'_{xz}\varepsilon'_{zy} \Big/ \varepsilon'_{zz}$$

$$\mathrm{H}_{22}(1,1) = -ik_y\varepsilon'_{yz} \Big/ \varepsilon'_{zz} - ik_x\mu_{zx} / \mu_{zz}$$

$$\mathbf{H}_{22}(1,2) = ik_x\varepsilon'_{yz} \Big/ \varepsilon'_{zz} - ik_x\mu_{zy} / \mu_{zz}$$

$$\mathbf{H}_{22}(2,1) = ik_y\varepsilon'_{xz} \Big/ \varepsilon'_{zz} - ik_y\mu_{zx} / \mu_{zz}$$

$$\mathbf{H}_{22}(2,2) = -ik_x\varepsilon'_{xz} \Big/ \varepsilon'_{zz} - ik_y\mu_{zy} / \mu_{zz}$$